

A Negative Activation Energy for Luminescence Decay: Specific Solvation Effects on the Emission Properties of Bis(2,2'-bipyridine)(3,5-dicarboxy-2,2'-bipyridine)ruthenium(II) Chloride

S. R. L. Fernando,^{†,‡} U. S. M. Maharroof,[†] Kurt D. Deshayes,^{†,‡}
Thomas H. Kinstle,[†] and Michael Y. Ogawa^{*,†,‡}

Contribution from the Department of Chemistry and Center for Photochemical Sciences,
Bowling Green State University, Bowling Green, Ohio 43403

Received November 29, 1995[⊗]

Abstract: A new mixed-ligand polypyridylruthenium(II) complex, [Ru(bpy)₂L]Cl₂, has been prepared where bpy = 2,2'-bipyridine and L = 3,5-dicarboxy-2,2'-bipyridine. The ligand L is a non-symmetrically-substituted 2,2'-bipyridine having two hydrophilic carboxylate groups located at the 3- and 5-positions of only one of its two pyridyl rings. In acetonitrile, the photophysical properties of the metal complex include a long-lived excited state ($\lambda_{em} = 637$ nm, $\tau = 846 \pm 11$ ns, $\phi = 0.046$ at 295 K) whose decay involves an activated crossing to higher energy ligand field states ($E_a = 4170 \pm 200$ cm⁻¹). This behavior is similar to that observed for other ruthenium tris(bipyridyl) compounds. In contrast, the title compound displays several unusual photophysical properties in aqueous solution. These include a strongly red-shifted emission ($\lambda_{em} = 685$ nm) having a short, pH-dependent lifetime which is quenched by an excited-state proton transfer from solvent. The completely deprotonated form of the molecule is the dominant emissive species. Surprisingly, under neutral conditions the excited-state lifetime increases with increasing temperature, from a value of $\tau = 54 \pm 1$ ns ($\lambda_{em} = 686$ nm, $\phi_{em} = 0.0036$) at 280 K to $\tau = 75 \pm 1$ ns ($\lambda_{em} = 675$ nm, $\phi_{em} = 0.0053$) at 360 K. The data are fit to the Arrhenius expression to give $E_a = -270 \pm 15$ cm⁻¹ in H₂O and $E_a = -178 \pm 10$ cm⁻¹ in D₂O. Thermochromic emission data and temperature-induced energy-gap law behavior indicate that the unique photophysical properties of this compound are due to specific interactions involving protic solvent.

Introduction

Understanding the role of specific solute–solvent interactions in the regulation of solution-phase photophysics has been a topic of considerable interest.¹ These phenomena provide the basis for the design of new molecules whose optical properties are highly sensitive to such important solvational factors as polarity, hydrogen-bonding ability, and viscosity. The use of such chemical species as probes of microsolvational environments has gained widespread importance in the physical characterization of polymers,² proteins,³ and synthetic inclusion complexes.^{4,5} For the past several decades, polypyridylruthenium(II) complexes have been widely studied because of their potential use in solar energy conversion schemes.^{6–8} Because so much is known about the photophysical properties of these com-

pounds, their continued study affords the opportunity to examine the physicochemical basis for the solvational control of excited states. This paper describes novel, solvent-dependent emission properties of a new ruthenium polypyridyl complex which can be attributed to specific interactions involving protic solvent. These properties include a strong solvatochromic red shift in emission, large solvent deuterium isotope effects in the emission lifetime, and decay rates that decrease with increasing temperature in aqueous solution.

In typical cases, photoexcitation of ruthenium polypyridyl complexes has been shown to generate a singlet metal-to-ligand charge-transfer state (¹MLCT) which undergoes rapid, highly efficient intersystem crossing ($\phi_{isc} \approx 1$) to a manifold of closely-spaced triplet states (³MLCT). These states have a relatively long-lived emission in aqueous solution ($\tau \approx 600$ ns). The mechanism for excited-state decay involves both radiative and nonradiative deactivation channels, in addition to a thermal population of high-lying ligand field (³LF) states.⁹ This last process gives rise to a distinctive temperature dependence of the excited-state lifetime which can be fit to a modified Arrhenius expression where the energy gap separating the ³MLCT and ³LF states falls within the range of 2500–4000 cm⁻¹.^{8c} Recent work¹⁰ has provided evidence for an additional

[†] Department of Chemistry.

[‡] Center for Photochemical Sciences.

[⊗] Abstract published in *Advance ACS Abstracts*, June 1, 1996.

(1) See for example: (a) Barbara, P. F.; Jarzaba, W. *Adv. Photochem.* **1990**, *15*, 1. (b) Reichardt, C. *Solvents and Solvent Effects in Organic Chemistry*; VCH: New York, 1988.

(2) See for example: *Photophysics of Polymers*; Hoyle, C. E., Torkelson, J. M., Eds.; ACS Symposium Series 358; American Chemical Society: Washington, DC, 1987.

(3) Negrierie, M.; Bellefeuille, S. M.; Whitham, S.; Petrich, J. W.; Thornburg, R. W. *J. Am. Chem. Soc.* **1990**, *112*, 7419.

(4) Diederich, F. *Cyclophanes*; Royal Society of Chemistry: Cambridge, 1991.

(5) Ponce, A.; Wong, P. A.; Way, J. J.; Nocera, D. G. *J. Phys. Chem.* **1993**, *97*, 11137.

(6) (a) DeArmond, M. K.; Hanck, K. W.; Wertz, D. W. *Coord. Chem. Rev.* **1985**, *64*, 65. (b) Kalyanasundaram, K. *Coord. Chem. Rev.* **1982**, *46*, 159. (c) Gratzel, M. *Acc. Chem. Res.* **1981**, *14*, 376.

(7) (a) Molnar, S. M.; Nallas, G.; Bridgewater, J. S.; Brewer, K. J. *J. Am. Chem. Soc.* **1994**, *116*, 5206. (b) Liska, P.; Vlachopoulos, N.; Nazeeruddin, Md.; Comte, P.; Gratzel, M. *J. Am. Chem. Soc.* **1988**, *110*, 3686.

(8) For a review, see: (a) Kalyanasundaram, K. *Photochemistry of Polypyridine and Porphyrin Complexes*; Academic: London, 1992. (b) Juris, A.; Balzani, V.; Barigelletti, F.; Campagna, S.; Belser, P.; Von Zelewsky, A. *Coord. Chem. Rev.* **1988**, *84*, 85. (c) Meyer, T. J. *Pure Appl. Chem.* **1986**, *58*, 1193.

(9) Van Houten, J.; Watts, R. J. *J. Am. Chem. Soc.* **1976**, *98*, 4853.

(10) (a) Sykora, M.; Kincaid, J. R. *Inorg. Chem.* **1995**, *34*, 5852. (b) Rillema, D. P.; Blanton, C. B.; Shaer, R. J.; Jackman, D. C.; Boldaji, M.; Bundy, S.; Worl, L. A.; Meyer, T. J. *Inorg. Chem.* **1992**, *31*, 1600. (c) Lumpkin, R. S.; Kober, E. M.; Worl, L. A.; Murtaza, Z.; Meyer, T. J. *J. Phys. Chem.* **1990**, *94*, 239.

thermally activated decay process that is thought to involve the population of a fourth, higher lying MLCT state having large singlet character and rapid rates of decay. For these cases, activation energies of 400–1000 cm^{-1} have been reported.¹⁰

In order to probe the effects of nonsymmetrical 2,2'-bipyridine ligands on the photophysical properties of polypyridylruthenium(II) compounds, we have prepared a novel mixed-ligand ruthenium polypyridyl complex, $[\text{Ru}(\text{bpy})_2\text{L}]$ where L is 3,5-dicarboxy-2,2'-bipyridine. A unique feature of this ligand is that it concentrates the effects of two hydrophilic carboxylate groups to one of its two pyridyl rings, creating a hydrophilic region of the molecule.¹¹ In acetonitrile, the photophysical properties of $[\text{Ru}(\text{bpy})_2\text{L}]$ closely resemble those of $[\text{Ru}(\text{bpy})_3]^{2+}$, including a long-lived excited state ($\tau = 846 \pm 11$ ns, $\phi = 0.046$ at 295 K) whose decay involves an activated crossing to higher energy LF states ($E_a = 4170 \pm 200$ cm^{-1}). However, in aqueous solution, the title compound displays several unusual photophysical properties which include a strongly red-shifted emission having a short, pH-dependent lifetime. Moreover, under neutral conditions the excited-state lifetime *increases with increasing temperature*, from a value of $\tau = 54 \pm 1$ ns at 280 K to $\tau = 75 \pm 1$ ns at 360 K. This behavior is accompanied by a noticeable blue shift in the emission maximum upon heating, and a decrease in k_{nr} in a manner that is in agreement with the energy-gap law. A strong solvent deuterium isotope effect is also observed in the temperature dependence of the excited-state lifetime. We interpret this behavior in terms of a deactivation process that involves specific interactions with protic solvent.

Experimental Section

General Methods. All chemicals and solvents were of reagent grade and used as received without further purification. $[\text{Ru}(\text{bpy})_3]\text{Cl}_2$ and $[\text{Ru}(\text{bpy})_2\text{Cl}_2]$ were purchased from Aldrich Chemicals. ¹H NMR spectra were recorded on either a Varian Unityplus 400 (400 MHz) or a Varian Gemini 200 (200 MHz) spectrometer. HPLC analyses were performed on a single pump system (Waters Model 510) equipped with a binary gradient controller (Autochrom Inc.) and a Waters Model 994 diode array detector/spectrophotometer. HPLC eluents consisted of helium-purged methanol/water gradients (20–40%) containing 0.1% (v/v) trifluoroacetic acid. UV/vis spectra were recorded on a Hewlett-Packard Model 8452A diode array spectrophotometer. GC/MS spectra were obtained on a Hewlett-Packard Model 5987A spectrometer. Cyclic voltammetry was conducted in distilled, argon-saturated acetonitrile (0.1 M tetrabutylammonium perchlorate) using a BAS 100W electrochemical analyzer with a platinum working electrode, a platinum wire auxiliary electrode, and a Ag/AgNO₃ reference electrode. Elemental analysis was obtained from Galbraith Laboratories, Inc. (Knoxville, TN).

Steady-State Emission Measurements. Steady-state emission measurements were recorded on a Spex Fluorolog fluorimeter equipped with two monochromators. The excitation wavelength (xenon lamp) was set to 488 nm which is an isosbestic point in the aqueous acid/base equilibria of the title compound. Corrections for detector sensitivity and background signals were performed for all spectra using the manufacturer's software routine. Emission quantum yields were calculated by comparison with the integrated intensity of the emission spectrum of an absorbance-matched solution of $[\text{Ru}(\text{bpy})_3]\text{Cl}_2$ ($\Phi_{\text{em}} = 0.042$).^{9,12}

Emission Lifetime Measurements. Emission lifetime measurements were obtained using a Q-switched Nd/YAG laser (Continuum, YG660). Most experiments used the 532 nm output (ca. 7 ns pulse width) with a diverging lens placed before the sample to expand the incident beam. In experiments used to determine the pH dependence of the emission lifetime, the 355 nm output was coupled to a tunable

laser system (OPOTEC Inc.) to generate a 488 nm excitation beam. A 700 nm interference filter (Oriel 57640) was placed before the entrance slit of the monochromator to remove scattered light. The emission at 700 nm was monitored using a computer-controlled kinetic spectrophotometer (Kinetic Instruments). Lifetime data and initial intensities of the decay curves were evaluated using PC RAD PROGRAM (Kinetic Instruments). Variable temperature experiments were achieved to ± 0.1 K using a water-jacketed cell holder connected to a thermostated circulating water bath equipped with an automated temperature controller. The temperatures of the solutions were directly measured using an alumel–chromel thermocouple. All lifetime measurements were performed in argon-saturated solutions to avoid possible complications arising from the presence of either oxygen or carbon dioxide in solution.

Acid/Base Titrations. The UV/vis and emission measurements obtained between $H_0 = 11$ and $H_0 = 0.6$ were performed on samples dissolved in 0.2 M NaCl. Ground-state absorption spectra were obtained from samples having an absorbance of ca. 0.5 at 488 nm. Emission measurements were performed on samples having an absorbance of ca. 1.6 at 488 nm, using front-face detection. The acidity of these solutions was adjusted by the addition of solutions of HCl and/or NaOH (0.1–8.0 M). Care was taken so that, throughout the entire procedure, the total volume change of the sample was negligible (<1%). The Hammett acidities (H_0) of these dilute solutions were assigned using a pH electrode calibrated in aqueous buffers and by assuming $\text{pH} = H_0$.¹³ In the strongly acidic regimes ($H_0 < 0.6$), absorption spectra were obtained by titrating with 98.6% H₂SO₄ and the data for the titration curve were obtained by preparing absorbance-matched solutions (516 nm) in aqueous sulfuric acid (2.26–28.7 wt %) having $H_0 = +0.48$ to -1.7 .¹³ Titration curves performed in D₂O ($H_0 = 7-1.6$) were obtained by dissolving the complex in 0.2 M NaCl in deuterium oxide (Isotec Inc., 99.9% atom) and adjusting the acidity with DCl (Aldrich, 99.5% atom).

Synthesis. 1,3,5-Trimethyl-2-pyridone (1). Methyl sulfate, 46.2 g (0.366 mol), was added dropwise to 39.2 g (0.366 mol) of 3,5-dimethylpyridine under an argon atmosphere with continuous stirring. This solution was heated overnight at 110 °C, cooled to room temperature, dissolved in 80 mL of H₂O, and cooled to 0 °C. To this stirring solution were simultaneously added solutions of 240 g (0.73 mol) of K₃Fe(CN)₆ in 480 mL of H₂O and 60 g (1.5 mol) of NaOH in 100 mL of H₂O dropwise from two separatory funnels. The addition rates were kept such that the reaction temperature never exceeded 5 °C. Addition of the NaOH solution was complete when 240 mL of the K₃Fe(CN)₆ had been added. After the addition of the remaining K₃Fe(CN)₆ solution the reaction mixture was allowed to warm to room temperature and stand for 5 h. The solution was extracted with CHCl₃ (3 × 100 mL), the organic layers were combined and dried with MgSO₄, and the solvent was removed under reduced pressure. Vacuum distillation of the resulting oil at 0.1 Torr and 90 °C gave 32.65 g (65%) of 1,3,5-trimethyl-2-pyridone (**1**) as a colorless liquid: ¹H NMR (200 MHz, CDCl₃) δ 7.1 (s, 1H), 6.9 (s, 1H), 3.5 (s, 3H), 2.1 (s, 3H), 2.0 (s, 3H); MS m/z (rel intens) 137 (M⁺, base), 108 (96), 94 (24).

2-Bromo-3,5-dimethylpyridine (2). To 30 g (110 mmol) of prewarmed (60 °C) PBr₃ under an argon atmosphere was added 3 g (21.8 mmol) of **1** dropwise. Once the addition was complete the solution was refluxed for 3 h. The reaction was subsequently cooled to room temperature, and the excess PBr₃ was removed via Kugelrohr distillation at 0.1 Torr and 50 °C. The residue was made strongly alkaline with 5% NaOH and added to 100 mL of CHCl₃. The inorganic material was removed by H₂O extraction (3 × 50 mL), and the organic layer was subsequently separated, dried with MgSO₄, and concentrated under reduced pressure. The resulting liquid was purified by Kugelrohr distillation at 0.1 Torr and 85 °C to give 2.65 g (68%) of 2-bromo-3,5-dimethylpyridine (**2**) as a yellow liquid: ¹H NMR (200 MHz, CDCl₃) δ 8.1 (s, 1H), 7.4 (s, 1H), 2.4 (s, 3H), 2.3 (s, 3H); MS m/z (rel intens) 187, 185 (M⁺), 106 (base), 79 (67), 77 (55).

Dimethyl 2-Pyridylboronate (3). To 375 mL of anhydrous THF under an argon atmosphere was added 5 mL (52.5 mmol) of 2-bromopyridine. The resulting solution was cooled to -78 °C. Using an air-tight syringe, 38 mL of 1.6 N *n*-BuLi in hexane was rapidly added to the stirring solution. The reaction mixture was allowed to stand for

(11) Maharroof, U. S. M. Masters Thesis, Bowling Green State University, Bowling Green, OH, 1995.

(12) Demas, J. N.; Crosby, G. A. *J. Phys. Chem.* **1971**, 75, 991.

(13) Rochester, C. H. *Acidity Functions*; Academic: New York, 1970.

1 h at -78°C . The lithiate was cannulated into 190 mL of anhydrous THF and 50 mL of trimethoxyborane (-78°C). The resulting mixture was kept for 1 h at -78°C and allowed to warm to room temperature. Removal of THF followed by repeated washing with CH_3OH (5×100 mL) gave 8.25 g (83%) of dimethyl 2-pyridylboronate (**3**) as a yellow solid that was carried on to the next reaction with no further purification: $^1\text{H NMR}$ (200 MHz, CDCl_3) δ 8.43 (d, 1H), 7.60 (m, 2H), 7.08 (m, 1H), 3.13 (s, 6H).

3,5-Dimethyl-2,2'-bipyridine (4). A mixture of 1 g (5.41 mmol) of **2**, 876 mg (15.6 mmol) of KOH, 550 mg (2.61 mmol) of $\text{Et}_4\text{N}^+\text{Br}^-$, and 817 mg (5.41 mmol) of **3** in 50 mL of benzene was degassed by bubbling argon through the refluxing solution for 30 min. To this solution was added 1.25 g of $\text{Pd}[\text{P}(\text{Ph})_3]_4$,¹⁴ and the reflux was continued overnight. After solvent was removed under reduced pressure, 25 mL of H_2O was added. Extraction with CHCl_3 (3×50 mL) followed by silica gel column chromatography ($\text{EtOAc}/\text{CHCl}_3$ (20:80)) and Kugelrohr distillation at 0.1 Torr and 120°C gave 600 mg (60%) of 3,5-dimethyl-2,2'-bipyridine (**4**) as a colorless liquid: $^1\text{H NMR}$ (400 MHz, CDCl_3) δ 8.66 (m, 1H), 8.34 (s, 1H), 7.76 (m, 2H), 7.37 (s, 1H), 7.23 (m, 1H), 2.25 (s, 3H), 2.23 (s, 3H).

Dipotassium 2,2'-Bipyridine-3,5-dicarboxylate (5). A solution of 600 mg (3.3 mmol) of **4** and 2.6 g KMnO_4 (17 mmol) was refluxed in 25 mL of water under an argon atmosphere overnight. The reaction was quenched by the addition of several milliliters of ethanol and allowed to cool to room temperature. The solid MnO_2 was removed by vacuum filtration, and the filtrate was extracted with CHCl_3 (3×50 mL). The aqueous layer was concentrated by rotary evaporation, and the resulting residue was purified by reversed-phase C_{18} column chromatography using 256 nm UV detection and neat H_2O as the eluent. The product band was concentrated to near dryness, and the product was precipitated by the addition of 2 mL of ethanol followed by 100 mL of diethyl ether to yield 440 mg (42%) of dipotassium 2,2'-bipyridine-3,5-dicarboxylate (**5**) as a white solid: $^1\text{H NMR}$ (400 MHz, D_2O) δ 9.03 (s, 1H), 8.65 (d, 1H), 8.38 (s, 1H), 7.97 (m, 1H), 7.79 (d, 1H), 7.55 (m, 1H).

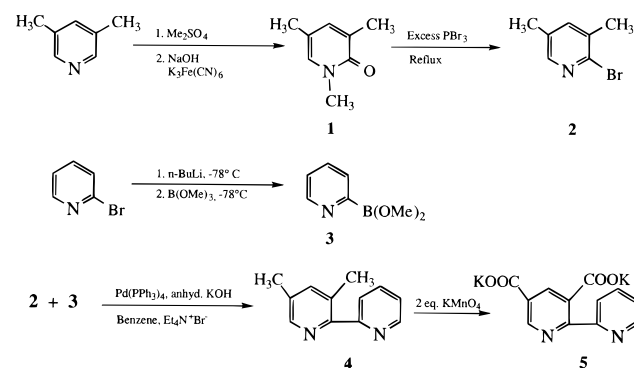
[Ru(bpy)₂L]Cl₂ (6). A solution of 100 mg (0.41 mmol) of **5** and 200 mg of $\text{Ru}(\text{bpy})_2\text{Cl}_2$ (0.41 mmol) in 50 mL of methanol was refluxed overnight under an argon blanket. The solution was allowed to cool to room temperature, and the solvent was then removed by rotary evaporation. Repeated reversed-phase C_{18} column chromatography (25% CH_3OH , 0.01% HCl eluent) afforded the pure product (160 mg, 50%) as determined by reversed-phase HPLC ($\text{CH}_3\text{OH}/\text{H}_2\text{O}$ gradients) using diode-array detection (290–600 nm). Anal. Calcd for $[\text{RuC}_{32}\text{H}_{24}\text{N}_6\text{O}_4]\text{Cl}_2 \cdot 2\text{H}_2\text{O}$: C, 50.3; H, 3.2; N, 11.0. Found: C, 50.3; H, 3.7; N, 11.0.

Results and Discussion

Synthesis. To our knowledge, relatively little work has been performed to develop an efficient synthesis of unsymmetrical 2,2'-bipyridine ligands. In this paper, we use a Suzuki cross-coupling reaction^{15,16} to prepare the unsymmetrical 3,5-dicarboxy-2,2'-bipyridine ligand **5** as shown in Scheme 1. This synthesis avoids the use of organostannane reagents commonly used in the preparation of unsymmetrical biaryls^{17–19} and involves the direct Pd(0)-catalyzed aryl–aryl coupling of boronic ester **3** and 2-bromo-3,5-dimethylpyridine **2**. The dimethyl compound **4** was then converted to the dicarboxylate **5** via KMnO_4 oxidation. Reaction of **5** with $\text{Ru}(\text{bpy})_2\text{Cl}_2$ yielded the complex $[\text{Ru}(\text{bpy})_2\text{L}]\text{Cl}_2$ used in the photophysical studies discussed below, $\text{L} = 3,5\text{-dicarboxy-2,2'-bipyridine}$.

Electrochemistry in Acetonitrile. In acetonitrile, the cyclic voltammogram of the deprotonated form of $[\text{Ru}(\text{bpy})_2\text{L}]$ consists

Scheme 1



of one reversible anodic wave centered at +1.01 V vs Ag/AgNO_3 and three reversible cathodic waves at -1.74 , -1.94 , and -2.25 V. These processes are assigned to the metal-centered oxidation and the three ligand-based reductions. We note that the oxidation process occurs at a potential similar to that of $[\text{Ru}(\text{bpy})_3]$, whereas the observed reduction potentials are shifted by ca. -0.1 V.²⁰

Ground-State Absorption and Emission Properties in Acetonitrile. The absorption spectrum of $[\text{Ru}(\text{bpy})_2\text{L}]$ dicarboxylate is very similar to that of $[\text{Ru}(\text{bpy})_3]^{2+}$ when taken in acetonitrile. Comparison of this spectrum with those of both $[\text{Ru}(\text{bpy})_3]^{2+}$ and the deprotonated free ligand (L^{2-}) affords assignment of the bands occurring at ca. 200 nm ($\log \epsilon = 4.71$) and 290 nm ($\log \epsilon = 4.72$) to ligand-centered $\pi-\pi^*$ transitions. Similarly, the bands at 244 nm ($\log \epsilon = 4.36$) and 460 nm ($\log \epsilon = 4.03$) are assigned to MLCT ($d-\pi^*$) transitions which are slightly red-shifted relative to those reported for $[\text{Ru}(\text{bpy})_3]^{2+}$. Acid/base titrations were used to confirm the protonation state of the molecule. The addition of either HClO_4 or HCl was seen to produce a broadening and red shift of both the MLCT absorption band and the emission spectrum of the compound (not shown). Back-titration with pyridine quantitatively regenerated the original spectrum taken in the neat solvent. These results are in agreement with the acid/base behavior observed in aqueous solution (vide infra) and show that $[\text{Ru}(\text{bpy})_2\text{L}]$ exists in its deprotonated form when dissolved in acetonitrile.

The emission properties of $[\text{Ru}(\text{bpy})_2\text{L}]$ were measured in argon-saturated acetonitrile at ambient temperature. The results are listed in Table 1 along with those previously reported for related polypyridylruthenium(II) compounds. As shown, the title compound emits at a longer wavelength than $[\text{Ru}(\text{bpy})_3]^{2+}$, and has a shorter emission lifetime and smaller quantum yield. The emission lifetime (τ_{obs}) of $[\text{Ru}(\text{bpy})_2\text{L}]$ is strongly temperature-dependent. A plot of $\ln k_{\text{obs}}$ vs $1/T$ (Figure 1) shows that $k_{\text{obs}} = 1/\tau_{\text{obs}}$ increases with increasing temperature within the range of 279–332 K, and the data produce a nonlinear Arrhenius curve. Similar behavior has been observed for other polypyridyl complexes of Ru(II) in which Scheme 2 has been used to describe the various deactivation channels for the emissive $^3\text{MLCT}$ state.^{8,9,21} In this scheme, k_r and k_{nr} are, respectively, the rate constants for the nominally temperature-independent radiative and nonradiative decay processes and k_0 refers to the dominant temperature-dependent deactivation pathway. These terms can be used to give eq 1 which is generally employed to

$$k_{\text{obs}} = [(k_r + k_{\text{nr}}) + k_0 \exp(-E_a/RT)] \quad (1)$$

quantify this behavior. According to Scheme 2, the temperature-

(14) Coulson, D. R. *Inorg. Synth.* **1990**, 28, 107.

(15) Miyaura, N.; Yanagi, T.; Suzuki, A. *Synth. Commun.* **1981**, 11, 513.

(16) Deshayes, K. D.; Broene, R. D.; Knobler, C. B.; Diederich, F. *J. Org. Chem.* **1991**, 56, 6787.

(17) Stille, J. K. *Angew. Chem., Int. Ed. Engl.* **1986**, 25, 508.

(18) Ghadiri, M. R.; Soares, C.; Choi, C. *J. Am. Chem. Soc.* **1992**, 114, 825.

(19) Yamamoto, Y.; Azuma, Y.; Mitoh, H. *Synthesis* **1986**, 564.

(20) Mabrouk, P. A.; Wrighton, M. S. *Inorg. Chem.* **1986**, 25, 526.

(21) (a) Cherry, W. R.; Henderson, L. J., Jr. *Inorg. Chem.* **1984**, 23, 983. (b) Henderson, L. J., Jr.; Cherry, W. R. *J. Photochem.* **1985**, 28, 143.

Table 1. Emission Properties of [Ru(bpy)₂L] Complexes in Water, Deuterium Oxide, and Acetonitrile Solvents

L	emission λ_{max} (nm) ^b			τ (ns) at RT			Φ_{em} at RT			E_a (cm ⁻¹)			k_H/k_D at RT
	H ₂ O	D ₂ O	AN	H ₂ O	D ₂ O	AN	H ₂ O	D ₂ O	AN	H ₂ O	D ₂ O	AN	
3,5-dcbpy ^a	685	680	637	56 ± 2	146 ± 2	846 ± 11	0.0038	0.0096	0.046	-270 ± 15	-178 ± 10	4170 ± 200	2.6
4,4'-dcbpy ^a	657	659 ^{21a}	657	434 ^d	993 ^d	1060	0.039 ²¹	0.084 ^{21a}	^c	4230 ^{21a}	4227 ^{16a}	^c	2.3
bpy	624	624	620	574	956	968	0.042 ⁹	0.095 ^{21a}	0.062 ³⁰	3559 ^{21a}	3603 ^{16a}	3800 ³⁰	1.7

^a Deprotonated dicarboxylate form. ^b Uncertainty ± 1 nm. ^c Data not available. ^d Due to discrepancies in the literature values previously reported for these values (ref 23a), lifetime measurements were performed on a fresh sample of [Ru(bpy)₂(4,4'-dcbpy)]Cl₂ which was extensively purified by reversed-phase C18 column chromatography.

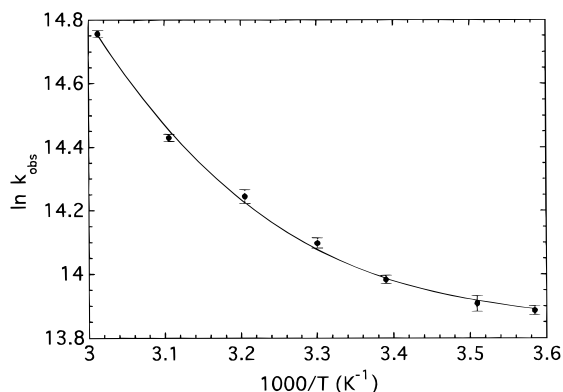


Figure 1. $\ln k_{\text{obs}}$ vs $1/T$ in argon-saturated CH₃CN. The solid line is calculated from the parameters obtained from fitting the data to eq 1. Error bars are evaluated from the uncertainties in lifetime measurements.

dependent decay channel is an activated surface crossing from the emissive ³MLCT state to a higher-lying ³LF state followed by rapid nonradiative decay to the ground state or ligand dissociation. When these states are not in thermal equilibrium, typical values are $k_r + k_{\text{nr}} = 10^6 \text{ s}^{-1}$, $k_0 = 10^{12} - 10^{14} \text{ s}^{-1}$, and $E_a = 2500 - 4500 \text{ cm}^{-1}$.^{10c} Analysis of the data presented in Figure 1 demonstrates that this behavior also obtains for the title compound. A nonlinear least squares fit of the data to eq 1 yields $k_r + k_{\text{nr}} = (1.03 \pm 0.03) \times 10^6 \text{ s}^{-1}$, $k_0 = (1.1 \pm 0.2) \times 10^{14} \text{ s}^{-1}$, and $E_a = 4170 \pm 200 \text{ cm}^{-1}$. Examination of the data presented in Table 1 shows that the difference in E_a determined for [Ru(bpy)₂L] and [Ru(bpy)₃]²⁺ is $\Delta E_a = 370 \pm 200 \text{ cm}^{-1}$, which can be reasonably attributed to their difference in room temperature emission energies, $\Delta E_{\text{em}} = -430 \pm 35 \text{ cm}^{-1}$ as predicted by Scheme 2. This result suggests that the energies of the LF states of these complexes are not significantly affected by the presence of the nonsymmetrical 2,2'-bipyridyl ligand (L).

At any temperature, the fractional contribution, $f(T)$ of the LF deactivation channel to the total excited-state decay process can be calculated using eq 2.⁹ Substitution of the kinetic

$$f(T) = \frac{k_0 \exp(-E_a/RT)}{[(k_r + k_{\text{nr}}) + k_0 \exp(-E_a/RT)]} \quad (2)$$

parameters obtained above gives $f(T) = 0.5$ at 298 K. Thus, at room temperature, the activated surface crossing to the LF states provides a significant contribution to the excited-state decay in acetonitrile.

Ground-State Absorption Spectra and Acid/Base Properties in Aqueous Solution. When dissolved in aqueous solution, the ground-state absorption properties of [Ru(bpy)₂L]Cl₂ are strongly dependent upon the acidity of the medium (Figure 2). The observed changes are completely reversible and stable for several days. At $H_0 > 4.5$, the low-energy MLCT band is located at 452 nm ($\log \epsilon = 4.06$) which coincides with the position of the MLCT band of [Ru(bpy)₃]²⁺. At higher acidities,

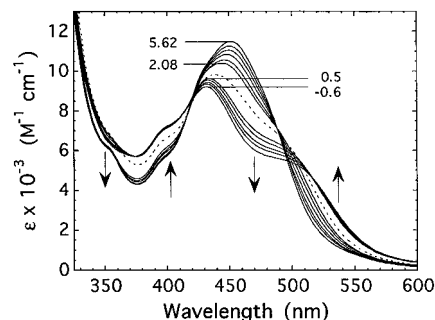
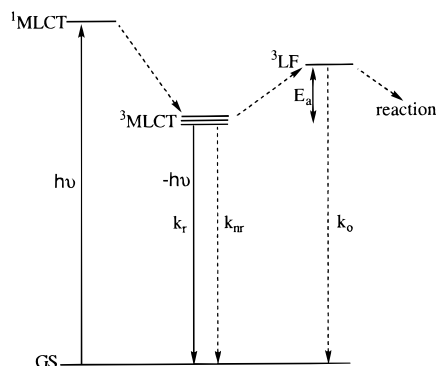


Figure 2. Acid/base dependence of the visible absorption spectra taken in aqueous solution at room temperature. Spectra were obtained at $H_0 = 5.62, 3.25, 2.93, 2.64, 2.35, 2.08, 1.27$ (dotted line), 0.50, 0.35, 0.12, -0.05, and -0.6. Note the loss of isosbestic behavior at $H_0 = 1.27$. The arrows indicate the direction of the spectral changes that occur in response to increasing acidity.

Scheme 2



this band loses intensity and a new, low-energy shoulder appears at ca. 500 nm. Similar behavior has been observed for [Ru(bpy)₂(dcbpy)]²⁺, dcbpy = 4,4'-dicarboxy-2,2'-bipyridine, where at low pH the presence of the electron-withdrawing carboxylic acid substituents inductively stabilizes the ³MLCT state of the complex.²²⁻²⁵

Throughout the entire acidity range studied, two sets of isosbestic points are seen in the absorption data, which demonstrates that two distinct protonation steps occur in the title compound. The first set of isosbestic points are observed between $H_0 = 11.0$ and $H_0 = 2.08$, and occur at 488 nm ($\log \epsilon = 3.86$), 416 nm ($\log \epsilon = 3.92$), and 356 nm ($\log \epsilon = 3.79$). The second set are seen at $H_0 < 0.5$ and occur at 516 nm ($\log \epsilon = 3.69$), 412 nm ($\log \epsilon = 3.91$), and 374 nm ($\log \epsilon = 3.78$). Isosbestic behavior is not observed at intermediate acidities (0.5

(22) (a) Kalyanasundaram, K.; Nazeeruddin, Md. K.; Gratzel, M.; Viscardi, G.; Savarino, P.; Barni, E. *Inorg. Chim. Acta.* **1992**, 198-200, 831. (b) Nazeeruddin, Md. K.; Kalyanasundaram, K. *Inorg. Chem.* **1989**, 28, 4251.

(23) (a) Lay, P. A.; Sasse, W. H. F. *Inorg. Chem.* **1984**, 23, 4123. (b) Ferguson, J.; Mau, A. W.-H.; Sasse, W. H. F. *Chem. Phys. Lett.* **1979**, 68, 21.

(24) Shimidzu, T.; Iyoda, T.; Izaki, K. *J. Phys. Chem.* **1985**, 89, 642.

(25) Giordano, P. J.; Bock, C. R.; Wrighton, M. S.; Interrante, L. V.; Williams, R. F. X. *J. Am. Chem. Soc.* **1977**, 99, 3187.

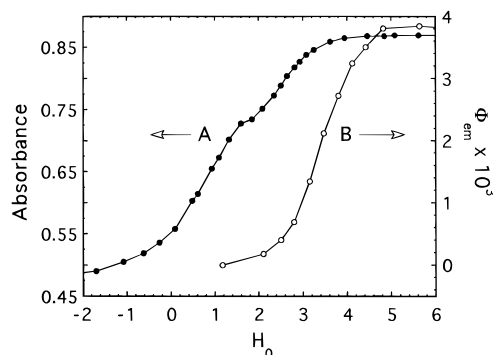


Figure 3. Ground- and excited-state acid/base titration curves taken in aqueous solution at room temperature: (A) absorbance at 460 nm taken within the range $-2.0 \leq H_0 \leq +6.0$, (B) emission quantum yields recorded within the range $1.2 \leq H_0 \leq 6.0$. In both cases, the titrations were carried out to $H_0 = 11$. However, the data obtained above $H_0 = 6.0$ are omitted from the figure since they show no further change with increased basicity.

Scheme 3



$< H_0 < 2.08$). These spectral changes are completely reversible, and the compound is stable at each acid strength. Figure 3 plots the absorption at $\lambda = 460$ nm as a function of H_0 . Two well-separated inflection points can be observed to give values of $\text{p}K_{a1} = 0.7$ and $\text{p}K_{a2} = 2.7$ for this compound. However, because the two carboxylic acid moieties of this compound are not symmetrically related, four separate acid/base equilibria might be expected. The observation of two regions of isosbestic behavior and two inflection points in the titration plot suggests that a simplified two-step equilibrium scheme (Scheme 3) can be used to describe the acid/base behavior of this compound. Here, **II** represents both of the monodeprotonated species, differing only in their site of protonation (i.e., both at the 3- and 5-carboxy positions).

The $\text{p}K_a$ values determined above can be compared to those reported for $[\text{Ru}(\text{bpy})_2(4,4'\text{-dcbpy})]^{2+}$: $\text{p}K_{a1} = 1.85$ and $\text{p}K_{a2} = 2.90$.²³ The stronger acidity of **I** as compared to its 4,4'-dcbpy analog can be attributed to the fact that its two electron-withdrawing carboxylic acid groups are more proximal than those present in 4,4'-dcbpy. Completion of the first deprotonation step minimizes this inductive effect to give comparable values of $\text{p}K_{a2}$ for the two compounds.

Acid/Base Dependence of the Emission Properties in Aqueous Solution. Under neutral conditions (295 K), the emission properties of $[\text{Ru}(\text{bpy})_2\text{L}]$ include a maximum at $\lambda_{\text{em}} = 685$ nm, a quantum yield of $\phi = 3.8 \times 10^{-3}$, and a lifetime of $\tau = 56 \pm 2$ ns (Table 1). The short lifetime and reduced quantum yield are consistent with the low energy of emission that this compound displays in water (vide infra). As shown in Figure 4, the emission properties are strongly acid-dependent. A reversible decrease in both ϕ and τ (lifetime data not shown) can be observed when the acidity is lowered below $H_0 = 4.5$. However, throughout the entire acidity range examined ($H_0 = 11-0.6$), the emission decay remains single exponential and no significant red shift in λ_{em} can be observed, except for an extremely weak emission that appears at $H_0 < 3$ ($\phi \leq 1.6 \times 10^{-4}$, $\lambda_{\text{em}} > 700$ nm). Thus, under neutral conditions, the only significantly emissive form of $[\text{Ru}(\text{bpy})_2\text{L}]$ is the completely deprotonated species **III***. This behavior may be compared to that of $[\text{Ru}(\text{bpy})_2(4,4'\text{-dcbpy})]$ in which all acid/base forms of the molecule are strongly luminescent, and where protonation

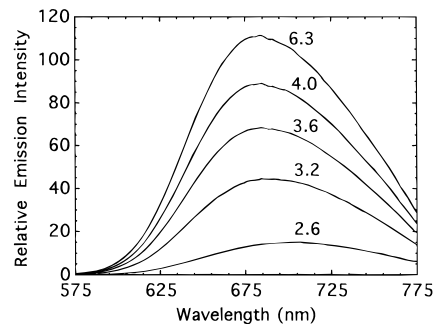


Figure 4. Acid/base dependence of the corrected emission spectra ($\lambda_{\text{irr}} = 488$ nm) taken in argon-saturated aqueous solution at room temperature. The curves correspond to $H_0 = 6.3, 4.0, 3.6, 3.2,$ and 2.6 .

of the two carboxylate groups produces both a red shift in λ_{em} and a substantial drop in emission intensity.^{21,23} The same general trend is observed for $[\text{Ru}(\text{bpy})_2\text{L}]$. However, because the $[\text{Ru}(\text{bpy})_2\text{L}]$ dicarboxylate is itself only weakly emissive, protonation results in an almost negligible emission occurring at > 700 nm, as seen in Figure 4.

The weak emission of the deprotonated $[\text{Ru}(\text{bpy})_2\text{L}]$ is likely due to the asymmetric substitution of the two carboxylate groups onto only one of the two pyridyl rings of **L**. This situation may serve to produce a strongly hydrophilic region of the molecule and enhance the degree of solvation of the excited charge-transfer state relative to that of either $[\text{Ru}(\text{bpy})_3]^{2+}$ or $[\text{Ru}(\text{bpy})_2(4,4'\text{-dcbpy})]$. Such strongly solvent-stabilized MLCT states would be expected to have a relatively short-lived and red-shifted emission in accordance with the energy-gap law (vide infra).

Figure 3 shows a plot of the emission quantum yield vs H_0 . The curve shows a single inflection point at $H_0 = 3.5$ to give an apparent value of $\text{p}K_a^*$ for the excited state. A similar plot of the emission lifetime data (not shown) shows nearly identical behavior within the low acidity regime. However, such data could not be collected at $H_0 < 2.5$ due to the time resolution of the instrumentation used. The higher apparent value for $\text{p}K_a^*$ as compared to the ground-state $\text{p}K_a$ (Figure 3) indicates that the excited-state species **III*** is a slightly stronger base than its ground-state analog **III**, as would be expected from the MLCT character of the excited state.²⁶

At this point, it is not clear whether the shape of the luminescence titration curve results from an excited-state equilibrium or a kinetically-controlled quenching process involving protons. To this end, Scheme 4 can be used to analyze the nature of the acid/base dependence of τ and ϕ where the site of protonation has been arbitrarily depicted as occurring at the 5-carboxy position of **L**. In order for the data to result from a true excited-state acid/base equilibrium, the excited-state protonation and deprotonation steps must occur rapidly as compared to the decay of the relevant excited states (i.e., $[\text{H}_3\text{O}^+]\text{k}^*_{+\text{H}} \gg k_0(\text{III}^*)$ and $\text{k}^*_{-\text{H}} \gg k_0(\text{II}^*)$).^{27,28} However, neither of these conditions are satisfied for the present case. Firstly, the observed lifetimes of **III*** are strongly H_0 -dependent, demonstrating that its rate of protonation is comparable to its rate of emission decay: $([\text{H}_3\text{O}^+]\text{k}^*_{+\text{H}} \approx k_0(\text{III}^*))$. Secondly, at low H_0 , the direct excitation of **II** produces very little observable emission ($\phi \leq 1.6 \times 10^{-4}$) which indicates that the deprotonation of **II*** is slow: $\text{k}^*_{-\text{H}} \ll k_0(\text{II}^*) \approx 10^8 \text{ s}^{-1}$. Thus, the

(26) Vos, J. G. *Polyhedron* **1992**, *11*, 2285.

(27) (a) Lasser, N.; Feitelson, J. J. *Phys. Chem.* **1973**, *77*, 1011. (b) Lasser, N.; Feitelson, J. J. *Phys. Chem.* **1975**, *79*, 1975.

(28) Mesmaeker, A. K-D.; Jacquet, L.; Nasielski, J. *Inorg. Chem.* **1988**, *27*, 4451.

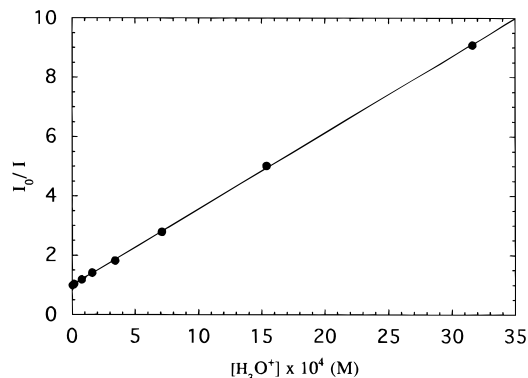
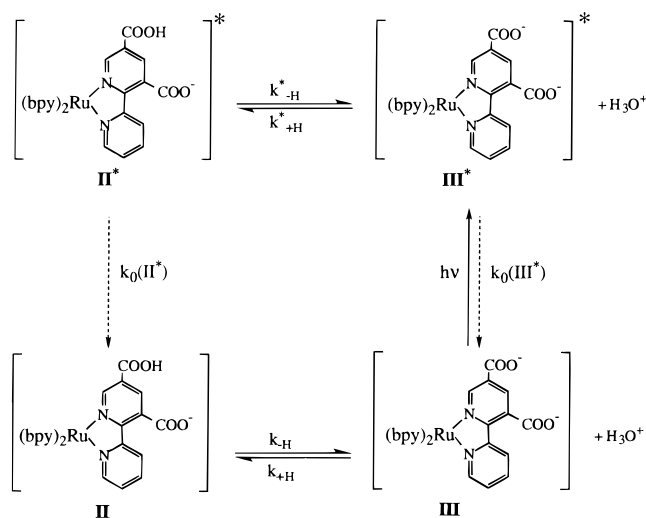


Figure 5. Stern–Volmer plot of the pH-dependent quenching of the emission intensity in argon-saturated aqueous solution at room temperature. I_0 and I are the emission intensities taken in the absence and presence of proton quenching, respectively.

Scheme 4



excited-state titration plot does not reflect the properties of a true acid/base excited-state equilibrium but rather results from a rate-limiting excited-state proton transfer to form the non-emissive species II^* .

The second-order rate constant for the excited-state proton transfer, k_{+H}^* , can be obtained by applying the steady-state approximation to Scheme 4 to give eq 3. Here, I_0 and I are,

$$\frac{I_0}{I} = \frac{1 + \tau_0(\text{III}^*)k_{+H}^*[\text{H}_3\text{O}^+]}{1 + k_{-H}^*\tau_0(\text{II}^*)} \quad (3)$$

respectively, the emission intensities taken in the absence and presence of proton quenching, and the excited state lifetimes are $\tau_0(\text{III}^*) = 1/k_0(\text{III}^*)$ and $\tau_0(\text{II}^*) = 1/k_0(\text{II}^*)$. Equation 3 can be rewritten in the form of the Stern–Volmer expression (eq 4), since $k_{-H}^*\tau_0(\text{II}^*) \ll 1$. Figure 5 shows a fit of the data

$$\frac{I_0}{I} = 1 + \tau_0(\text{III}^*)k_{+H}^*[\text{H}_3\text{O}^+] \quad (4)$$

to eq 4 using $\tau_0(\text{III}^*) = 56$ ns to give the rate of excited-state proton transfer as $k_{+H}^* = 4 \times 10^{10} \text{ M}^{-1} \text{ s}^{-1}$. These results can be confirmed by fitting the emission lifetime data to eq 5 (not

$$\frac{1}{\tau_{\text{obs}}} = \frac{1}{\tau_0(\text{III}^*)} + k_{+H}^*[\text{H}_3\text{O}^+] \quad (5)$$

shown) which yields values of $k_{+H}^* = 3 \times 10^{10} \text{ M}^{-1} \text{ s}^{-1}$ and

$\tau_0(\text{III}^*) = 59$ ns, close to the experimentally determined value. A similar treatment of the steady-state emission data obtained in D_2O yields $k_{+D}^* = 2 \times 10^{10} \text{ M}^{-1} \text{ s}^{-1}$.

In summary, analysis of the acid/base dependence of the emission lifetime and quantum yield data shows that the excited-state species III^* is quenched by a diffusion-controlled proton transfer in a manner similar to that reported for related $\text{Ru}(\text{II})$ compounds.²⁹

Temperature Dependence of the Emission Properties in Aqueous Solution. As compared to the room-temperature spectrum obtained in acetonitrile ($\lambda_{\text{em}} = 637$ nm), the emission spectrum of $[\text{Ru}(\text{bpy})_2\text{L}]$ taken in unbuffered aqueous solution displays a strong solvatochromic shift to lower energy ($\lambda_{\text{em}} = 685$ nm). While similar behavior has been reported for some related ruthenium tris(diimine) complexes, it is of interest to note that the shift seen for the title compound is among the largest reported.^{8b,30,31} Emission spectra obtained in H_2O , D_2O , CH_3OH , CD_3OD , and $\text{CF}_3\text{CH}_2\text{OH}$ show no obvious correlation between λ_{em} and solvent polarity.³² However, the emission maxima observed in these protic media uniformly occur at lower energies than that seen in acetonitrile. Thus, interactions with protic solvent are suspected to play an important role in regulating the photophysical properties of $[\text{Ru}(\text{bpy})_2\text{L}]$. Consistent with this is the observation of a strong solvent deuterium isotope effect on τ . At 295 K, the emission lifetime is $\tau = 56 \pm 2$ ns in argon-saturated H_2O which increases to a value of $\tau = 146 \pm 2$ ns in argon-saturated D_2O ($k_{\text{H}}/k_{\text{D}} = 2.6$). This solvent isotope effect is nearly independent of temperature (278–333 K) and larger than that observed at room temperature for either $[\text{Ru}(\text{bpy})_2(4,4'\text{-dcbpy})]$ ($k_{\text{H}}/k_{\text{D}} = 2.3$) or $[\text{Ru}(\text{bpy})_3]^{2+}$ ($k_{\text{H}}/k_{\text{D}} = 1.7$).^{9,21a} It is interesting to note that, for $[\text{Ru}(\text{bpy})_3]^{2+}$, the solvent isotope effect is nearly eliminated at high temperature (368 K).⁹ Apparently, the molecular basis for the isotope effect in $[\text{Ru}(\text{bpy})_2\text{L}]$ is different from that in $[\text{Ru}(\text{bpy})_3]^{2+}$.

The substantial solvatochromic red shift in the emission of $[\text{Ru}(\text{bpy})_2\text{L}]$ reflects a lowering of the emissive $^3\text{MLCT}$ states by over 10^3 cm^{-1} as compared to the value in acetonitrile. This situation can be expected to strongly influence the mechanism for excited-state decay (Scheme 2) since the energies of the excited metal-centered LF states are generally assumed to be independent of solvent due to their negligible change in dipole moments.^{30,31} Thus, it is expected that thermal access to the deactivating ^3LF states would be substantially reduced in aqueous solution to yield a temperature dependence of k_{obs} different from that previously described in acetonitrile.

Figure 6 shows the temperature dependence of τ taken in unbuffered, argon-saturated water. As shown, the lifetimes do indeed exhibit a temperature response different from that seen in Figure 1. Most interestingly, the emission lifetimes in water increase with increasing temperature from $\tau = 54 \pm 1$ ns at 280 K to $\tau = 75 \pm 1$ ns at 360 K. Such behavior is clearly inconsistent with the schemes typically used to describe the excited-state decay of ruthenium polypyridyl compounds. To better characterize the magnitude of the unusual temperature dependence of k_{obs} , the data were fit to the Arrhenius expression $k_{\text{obs}} = A_0 \exp(-E_a/RT)$ to give a preexponential rate constant of $A_0 = (4.6 \pm 0.1) \times 10^6 \text{ s}^{-1}$ and a negative activation energy of $E_a = -270 \pm 15 \text{ cm}^{-1}$. The results of this fit are in reasonably good agreement with the experimental data, as seen in the inset to Figure 6. Data obtained in D_2O yield qualitatively similar behavior (not shown) but with a distinctly smaller

(29) Sun, H.; Hoffman, M. Z. *J. Phys. Chem.* **1993**, *97*, 5014.

(30) Caspar, J. V.; Meyer, T. J. *J. Am. Chem. Soc.* **1983**, *105*, 5583.

(31) Sun, H.; Hoffman, M. Z. *J. Phys. Chem.* **1993**, *97*, 11956.

(32) The emission maxima taken in the alcoholic solvents at 295 K occur at $\lambda_{\text{em}} = 651 \pm 2$ nm.

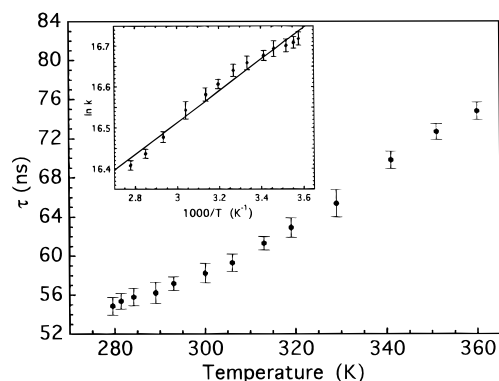


Figure 6. Temperature dependence of the emission lifetimes in argon-saturated aqueous solutions. Inset: data plotted in the form of $\ln k$ vs. $1/T$.

temperature dependence: $A_0 = (2.8 \pm 0.1) \times 10^6 \text{ s}^{-1}$ and $E_a = -178 \pm 10 \text{ cm}^{-1}$.

At this point, we note that the emission lifetimes of $[\text{Ru}(\text{bpy})_2\text{L}]$ observed in aqueous solution are much shorter than those seen for typical ruthenium polypyridyl compounds.^{8b} The observed lifetimes are independent of concentration (3×10^{-6} to $1 \times 10^{-4} \text{ M}$) and cannot be altered by purging the solution with argon gas. Thus, it is unlikely that the weakened emission results from a quenching process that involves either impurities or molecular oxygen. Rather, the red-shifted emission, diminished quantum yield, and shortened lifetimes are intrinsic properties of the complex. From the data presented in Table 1 (295 K), $k_r = (\phi/\tau)_{\text{obs}} = 6.8 \times 10^4 \text{ s}^{-1}$ and $k_{\text{nr}} = (k_{\text{obs}} - k_r) = 1.7 \times 10^7 \text{ s}^{-1}$, which shows that efficient nonradiative deactivation processes are responsible for the short excited-state lifetime. Thus, it is reasonable to conclude that any mechanism responsible for controlling the temperature dependence of τ acts by influencing the magnitude of k_{nr} .

In order to determine how temperature can be used to regulate the rates of nonradiative decay, steady-state emission spectra were obtained within the temperature range of 280–360 K. A distinct thermochromism was observed as the emission maximum moved from $\lambda_{\text{em}} = 686 \text{ nm}$ to $\lambda_{\text{em}} = 675 \text{ nm}$ upon heating which was accompanied by an increase in quantum yield from $\phi_{\text{em}} = 0.0036$ to $\phi_{\text{em}} = 0.0053$. Such behavior appears to be consistent with the energy-gap law for radiationless transitions which states that k_{nr} (and thus $1/\phi_{\text{em}}$) should vary exponentially with emission energy according to eq 6, where A , B , and C are

$$\ln k_{\text{nr}} = [A + B\chi_0 - CE_{\text{em}}] \quad (6)$$

positive constants and χ_0 is related to the solvent reorganization energy.³³ To verify that the temperature dependence of k_{nr} does indeed result from thermally induced changes in E_{em} , the thermochromic emission data were used to generate the energy-gap law plots shown in Figure 7.³⁴ As seen, a linear relationship between $\ln k_{\text{nr}}$ and E_{em} was obtained in both H_2O and D_2O . It is interesting to note that the two energy-gap law plots have different y intercepts which implies that these two solvents have different solvent reorganization energies in a manner that cannot be explained in terms of the continuum model. Similar behavior has been observed previously by Meyer and co-workers.^{30,33} Thus, the unusual temperature dependence of k_{nr} , and therefore the emission lifetime, can indeed be attributed to thermally-

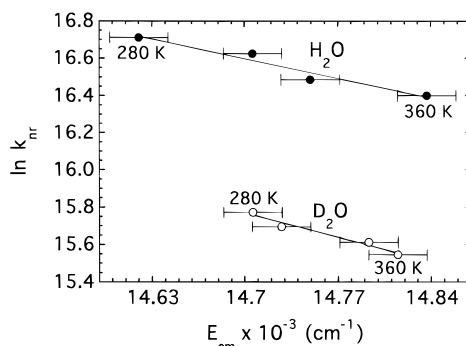


Figure 7. Temperature-induced energy-gap law plots in argon-saturated H_2O and D_2O taken in the range $280 \leq T < 360 \text{ K}$. Nonradiative decay rates were determined from the equation $k_{\text{nr}}(T) = [k_{\text{obs}}(T) - k_r(T)]$, where $k_r(T) = [\phi(T)/\tau(T)]$, and the relevant data were obtained from variable temperature lifetime and quantum yield measurements. Error bars correspond to $\pm 1 \text{ nm}$ uncertainty in emission peak maxima.

induced changes occurring within the degree of solvent stabilization of the emitting $^3\text{MLCT}$ states: at higher temperatures the emitting states become more weakly solvated to give elevated emission energies and longer emission lifetimes. The data presented in Figure 7 show that the emission spectra taken in D_2O exhibit a somewhat weaker thermochromism than those obtained in H_2O . This observation is consistent with the smaller magnitude of $-E_a$ seen in the deuterated solvent, and indicates that interactions involving solvent protons are involved in producing the thermochromic shifts in emission, and thus the negative activation energies for emission decay.

In summary, the emission properties of $[\text{Ru}(\text{bpy})_2\text{L}]$ are strongly solvent-dependent. Most notably, the emission lifetime increases with increasing temperature in aqueous solution. Such behavior cannot be explained in terms of either an activated surface crossing to high-lying LF states or the thermal population of a high-energy MLCT state as each of these models predicts a positive activation energy for excited-state decay. At this point, several statements can be made concerning the solvational microenvironment of $[\text{Ru}(\text{bpy})_2\text{L}]$ which appears to cause the unusual temperature behavior of k_{obs} . Firstly, the solvent deuterium isotope effects seen for λ_{em} , k_{obs} , $-E_a$, χ_0 , and the degree of thermochromicity suggest that the emission properties of $[\text{Ru}(\text{bpy})_2\text{L}]$ are strongly influenced by interactions involving solvent protons. This situation is consistent with quenching mechanisms involving either intra- or intermolecular hydrogen bonds as reported in both organic^{35–38} and inorganic systems.³⁹ Secondly, our recent studies suggest that the negative activation behavior does not depend upon the hydrogen-bond-donating ability of the solvent. Experiments performed in the strongly hydrogen-bonding solvent 2,2,2-trifluoroethanol ($T = 233\text{--}300 \text{ K}$) yield a value of $E_a = -220 \text{ cm}^{-1}$ which is very similar to that observed in H_2O .⁴⁰ Similarly, lifetime data obtained below 300 K in CH_3OH yield activation energies of $E_a = -300 \pm 15 \text{ cm}^{-1}$.⁴¹ These results suggest that specific solute–solvent hydrogen bonds are not the dominant force in regulating the

(35) Lin, S.; Struve, W. S. *Photochem. Photobiol.* **1990**, *54*, 361.

(36) Flom, S. R.; Barbara, P. F. *J. Phys. Chem.* **1985**, *89*, 4489.

(37) Inoue, H.; Hida, M.; Nakashima, N.; Yoshihara, K. *J. Phys. Chem.* **1982**, *86*, 3184.

(38) Miyasaka, H.; Mataga, N. In *Dynamics and Mechanisms of Photoinduced Transfer and Related Phenomena*; Mataga, N., Okada, T., Masuhara, H., Eds.; Elsevier: New York, 1992; pp 155–167.

(39) Turro, C.; Bossmann, S. H.; Jenkins, Y.; Barton, J. K.; Turro, N. J. *J. Am. Chem. Soc.* **1995**, *117*, 9026.

(40) Fernando, S. R. L.; Ogawa, M. Y. Unpublished data.

(41) Fernando, S. R. L.; Ogawa, M. Y. *Chem. Commun.* **1996**, 637.

(42) Bargelletti, F.; Juris, A.; Balzani, V.; Belser, P.; von Zelewsky, A. *J. Phys. Chem.* **1986**, *90*, 5190.

(33) Caspar, J. V.; Sullivan, B. P.; Kober, E. M.; Meyer, T. J. *Chem. Phys. Lett.* **1982**, *91*, 91.

(34) Because the temperature dependence measurements were performed in neutral solution on the deprotonated species III^* , the increase in emission lifetime cannot be due to a temperature variation in either $\text{p}K_a$ or $\text{p}K_a^*$: protonation of III^* can only serve to quench its emission.

emission properties of $[\text{Ru}(\text{bpy})_2\text{L}]$. Thirdly, the magnitudes of $| -E_a |$ observed in these studies are very small, being an order of magnitude smaller than the strengths of typical hydrogen bonds. Thus, the unusual behavior of $[\text{Ru}(\text{bpy})_2\text{L}]$ may reflect small temperature-induced fluctuations occurring within the solvational microenvironment of the molecule, and therefore be related to the solvent reorganization energy. If so, these results could lead to further insight into how solvational effects can generally influence the emission properties of charge-transfer states, and may have implications for interpreting the temperature behavior of some related ruthenium polypyridyl compounds.^{10,42} To further understand the fundamental nature of the solvational environment of $[\text{Ru}(\text{bpy})_2\text{L}]$, experiments are planned to (1) study the solvational dynamics of this system in a variety of different media and (2) probe the effects of altering the nature of the hydrophilic substituents of the complex. Future results from these studies may provide further insight into the

mechanisms for the solvational control of the excited-state properties of this and related molecules.

Acknowledgment. The authors thank Dr. James Wishart and Professors G. S. Hammond and M. A. J. Rodgers for helpful discussions. Professor Rodgers and Dr. W. Ford are also thanked for assistance in using the laser flash photolysis facilities at the Center for Photochemical Sciences. M.Y.O. gratefully acknowledges the National Science Foundation (Grant CHE-9307791), the donors of the Petroleum Research Fund (Grant G-25695), and the BGSU Faculty Research Committee for partially supporting this work. The National Science Foundation (Grant CHE-9302619) and Ohio Board of Regents Action Fund are also acknowledged for assisting in the purchase of the high-field NMR instruments at BGSU. Mr. J. Knauer is acknowledged for preliminary synthetic studies.

JA954015M